ELSEVIER

Journal of Power Sources 103 (2001) 18–24

JOURNAL OF POWER SOURCES

www.elsevier.com/locate/jpowsour

Characteristics of electrodes materials and their lifetime modeling for AMTEC

M.A.K. Lodhi*, M.S. Chowdhury[1]

Department of Physics, Texas Tech University, Lubbock, TX 79409, USA

Received 7 May 2001; accepted 20 May 2001

Abstract

One major problem in the power output of alkali metal thermal to electric converter (AMTEC) is its decay with time. From the 18,000 h of laboratory testing on AMTEC, it was found that power output decreased from 2.48 to 1.27 W. One of the major causes of this decay is the grain growth of the electrodes. In this study, three electrodes have been studied in terms of their grain growth and a comparison of their performance has been made. Materials for those three electrodes, namely, RhW, Rh_2W, and TiN have been tried. From this analysis, RhW was found to be the best electrode, whereas Rh_2W was found to be the better electrode over TiN electrode. It was observed that power degradation of RhW electrode is 3.63% from grain growth effect. Power degradation by Rh_2W and TiN electrodes were calculated to be 6.45 and 10.89%, respectively, due to grain growth.

Keywords: AMTEC; Electrode; Power degradation; Time dependency; Grain size growth

1. Introduction

Alkali metal thermal to electric converter (AMTEC) has been a candidate for space power as a thermal to electric converter. One of the reasons for AMTEC being used is its high efficiency over other conventional thermal to electric converter. However, there is still some problem associated with its long and continuous use. Power output of the device is yet to perform consistently with time. During the testing of the AMTEC in the laboratory, it was seen that power output decreased from 2.48 to 1.27 W after 18,000 h of operation with the hot side temperature of 1023 K and the condenser side temperature of 600 K [1]. Recent study shows that beta alumina solid electrolyte (BASE) and electrodes are two of the most degrading components in the AMTEC [2,3]. The PX-3A version of AMTEC was used for those analyses. AMTEC is a thermal to electric converter, which does not have any moving parts [4–7]. Sodium is working fluid and BASE is the ionic conductor.

BASE divides the AMTEC into two regions; a hot region filled with sodium at high-pressures (10–100 kPa) and high-temperatures (900–1300 K) and a cold region at low-pressures (<50 Pa) and low-temperatures (400–700 K) [8]. A porous metal electrode (cathode) covers the low-pressure (outer) side of the BASE. The anode surface covers the inner side of the BASE at the high-pressure–temperature region of the cell (see Fig. 1). Both electrodes provide a conduction path for the electrons to and from the external load. Sodium enters the hot region of the cell. Due to the thermodynamic potential across the BASE, ionization of sodium metal occurs at the hot region of sodium and BASE interface. The following reaction occurs at the interface of BASE and anode electrode surface [9]:

$$\mathrm{Na\,(vapor)} \rightarrow \mathrm{e^-} + [\mathrm{Na^+}] \quad (1)$$

The sodium ions are diffused through the BASE to the cathode due to the pressure differential across the BASE. The electrons circulate through the external load producing electrical work and then reach the cathode surface where they recombine with the sodium ions at the interface between the BASE and cathode.

The following reaction occurs at the interface of BASE and cathode surface [9]:

$$[\mathrm{Na^+}] + \mathrm{e^-} \rightarrow \mathrm{Na\,(vapor)} \quad (2)$$

The neutralized sodium leaves the porous electrode, moves through the vapor space, and releases their heat of condensation on the condenser surface. Nearly the entire temperature drop occurs in this low-pressure vapor space. The

* Corresponding author. Tel.: +1-806-742-3778; fax: +1-806-742-1182.
E-mail address: b5mak@ttacs.ttu.edu (M.A.K. Lodhi).
[1] Present address: 5599 TT Schlumerger, Suit no. 1040, San Felipe, Houston, TX 77056, USA.

0378-7753/01/$ – see front matter
PII: S0378-7753(01)00814-X

Nomenclature

B	temperature-independent exchange current (A $K^{1/2}$/Pa $m^{1/2}$)
c	proportionality constant
E	cell interface potential: applied potential+ voltage drop across cell resistance (V)
E_A	activation energy for grains to move to the grain boundary
F	Faraday constant
j	current density (A/cm^2)
M_0	mobility constant
n	constant, characteristic of the electrode material
P_e	power output (W)
P_1	pressure caused by the condensation of sodium from the condenser (Pa)
P_V	vapor pressure of sodium at the electrode temperature (Pa)
P_k	pressure due to sodium leaving the exterior surface of the electrode (Pa)
R_f	final grain size
R_0	initial grain size
R	gas constant
T	electrode temperature (K)

Greek letters

α	transfer coefficient = 0.5
γ_s	individual surface energy of the grain boundary
ϕ	angle by which two grains are separated
ΔP	pressure drop from the electrode–electrolyte interface to the electrode surface (Pa)

condensed liquid sodium moves to the wick annulus to the inlet of a small dc electromagnetic pump or a porous capillary wick, which is used to return the sodium to the high-pressure evaporator region.

For this study, three different materials for electrodes have been chosen to investigate their effect on the degradation of the overall power output. The electrodes were made of TiN, RhW, and Rh_2W materials. To simulate and investigate the time-dependent behavior of the three electrodes, an 18,000-line FORTRAN code was used. This code was based on the four models, namely (1) electrochemical model, (2) vapor pressure loss model, (3) electrical model, and (4) thermal model. The description of the four models can be found in ref. [10,11]. In this study, steady-state FORTRAN code was transformed into providing both steady and unsteady-state behavior and simulation was done on three different electrodes to investigate their grain size growth, time independent exchange current, and power output behavior with time.

2. Grain growth effect of electrode

The lifetime of an AMTEC electrode is dependent on the sintering rate of the material, which, is a function of the operating temperature of the cell. As the operating temperature increases, the sintering rate of the electrode also increases. As grains sinter, they coalesce, resulting in an increase in the grain volume. However, as the grains coalesce, porosity of the electrode increases and the surface area of the electrode decrease. The performance of the electrode is also related to the contact between electrode and electrolyte, which is measured by temperature-independent exchange current or just exchange current.

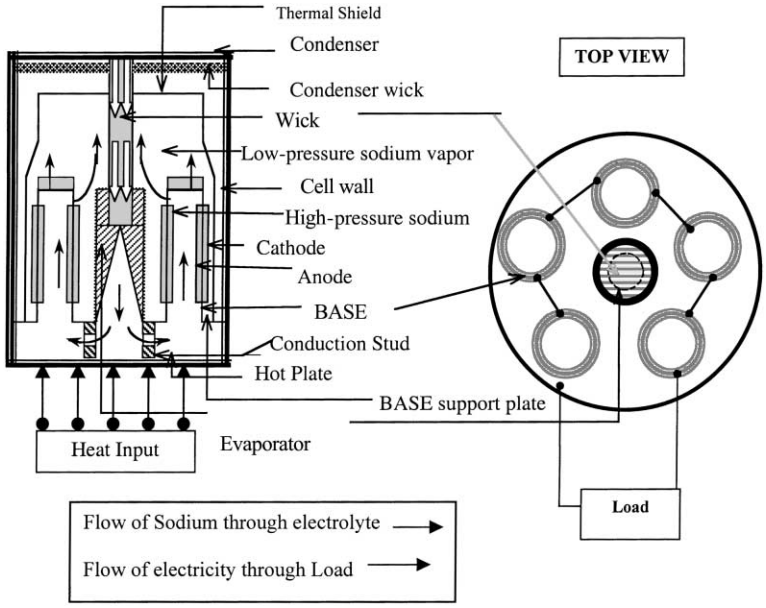

Fig. 1. Top and cross-sectional views of the PX-3A cell.

The exchange current depends on the sodium pressure at the interface of electrolyte and electrode. The sodium pressure at the interface is the sum of the pressure caused by the condensation of sodium from the condenser, the pressure due to sodium leaving the exterior surface of the electrode, and the pressure drop from the electrode–electrolyte interface to the electrode surface.

Exchange current can be calculated from the following relations [8,10]:

$$J_o^0 = j\left\{ e^{-\alpha Ef} - \frac{P_1 + P_k + \Delta P}{P_V} e^{(1-\alpha)Ef} \right\}^{-1} \quad (3)$$

$$f = \frac{F}{RT} \quad (4)$$

This exchange current is normalized for sodium collision rate to yield a temperature-independent exchange current [10]

$$B = J_o^0 \frac{T^{1/2}}{P_2} \quad (5)$$

Therefore, temperature-independent exchange current is a sensitive measure of the nature of contact between electrode and electrolyte interface. It can also be related with the operable lifetime of the electrode through grain radius.

With an increase in sintering, grain size increases, which eventually leads to a decrease in the number of grains. Therefore, contact between electrolyte and electrode also decreases. As the total number of grain decreases, the exchange current also decreases, because the exchange current is proportional to the number of grains in the electrode. With the increase of grain size, voids within the electrode become larger which causes the electrode conductivity to decrease. Eventually, these voids will grow to a huge size that there will be no apparent grain-to-grain conduction and the effective lifetime of electrode will cease.

3. Time-dependent equation for power output

In the previous sections, it was discussed that grain size was the primary mechanisms behind the electrode performance and power degradation. One idea to improve the electrodes is to use materials, which are less susceptible to the grain size growth effect. Since high-temperatures favor and accelerate the sintering and grain growth of material, it is logical to use materials, which have a higher melting point so that even at higher temperatures, they will be less susceptible to the grain size growth effect than those materials having a lower melting point.

Another criterion for the selection of an electrode material is its surface self-diffusion coefficient. Materials having low surface self-diffusion exhibit slow decay and grain growth would be slow. Therefore, materials having small surface self-diffusion coefficients and higher melting point temperatures should be sought and employed for better-expected results.

Table 1
Parameters of three electrodes

Electrode material	Activation energy (E_A) (kJ/mol)	a
TiN	175.5	1.14×10^{12}
RhW	260.51	4.3×10^{12}
Rh_2W	206.48	4.34×10^{12}

TiN, RhW, and Rh_2W materials meet all the criteria described above. In order to compare the performance of these three-electrode materials, it is necessary to find out the grain size growth effect of each of these electrode materials with time. The modeling of grain size growth by Ryan et al. [10] is used in this study in order to find out the grain growth of all three electrodes. The equation for grain growth is given by [11]

$$R_f = R_0 \left[1 + a \exp \frac{(-E_A/RT)t}{R_0^n} \right]^{1/n} \quad (6)$$

where

$$a = 2cM_0\gamma_s \cos\phi \quad (7)$$

The value of T, R, R_0 and n are 1023 K, 8.314 J/mol, 30 nm and 3.2, respectively. The following information in the Table 1 is also required for the development of equations for other electrode materials [11–13].

Using the values of a, T, R, R_0, n and Table 1 for all three electrodes, we get three equations for grain growth of the electrodes. The grain size growth of the materials investigated can be represented as, for TiN

$$R_f = 30[1 + 2.34 \times 10^{-2} t]^{0.3125} \quad (8)$$

for RhW

$$R_f = 30[1 + 4.06 \times 10^{-6} t]^{0.3125} \quad (9)$$

for Rh_2W

$$R_f = 30[1 + 2.33 \times 10^{-3} t]^{0.3125} \quad (10)$$

An empirical correlation between grain size and temperature-independent exchange current, B is given by [13]

$$B = B_0 - bR_f^{1/2} \quad (11)$$

B_0 is the initial temperature exchange current, which is equal to 270A $K^{1/2}$/Pa $m^{1/2}$. The values of b are 6.218 and 5.4222 for TiN and Rh_xW electrodes, respectively, found experimentally [13].

The temperature-independent exchange current as a function of grain growth for TiN and Rh_xW electrodes are as follows, respectively:

$$B = 270 - 6.218\,(R_f)^{1/2} \quad (12)$$

$$B = 270 - 5.4222\,(R_f)^{1/2} \quad (13)$$

The relation between temperature-independent exchange current, B, and power output can be found from the simulation work done in this study (see Appendix A). It is seen that as the temperature-independent exchange current increases, power output also increases at a given porosity and electrode material (TiN). From the simulation of FORTRAN code, the following relation has been obtained between the power output and temperature-independent exchange current (see Appendix A)

$$P_e = 1.5135 + 0.006B - 10^{-(1/2)B^2}. \quad (14)$$

For a given value of t, three Eqs. (8), (12), and (14) can be easily solved yielding three unknowns namely P_e, B, and, R_f. This gives the simulated relation between the power output and time for TiN electrode. Similarly, solving Eqs. (9), (13), and (14), simulated relation between power output and time for RhW electrode is found. The last simulated power output–time relation for Rh_2W electrode is obtained by solving Eqs. (10), (13), and (14).

4. Results and discussions

By solving the above equations, three relations between grain size, temperature-independent exchange current, and power output with time are obtained. The time-dependent behavior of the grain size for all three-electrode materials is shown in Fig. 2. Similarly, the unsteady-state behavior

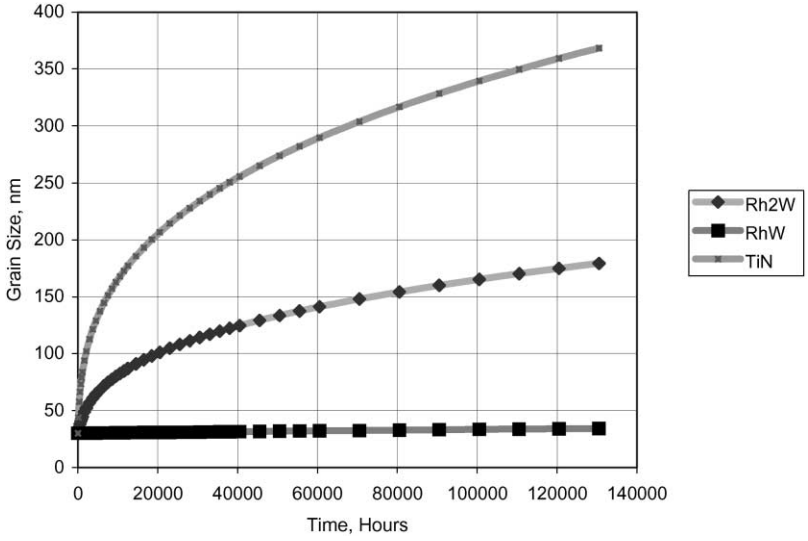

Fig. 2. The variation of grain size with time for RhW, Rh_2W, and TiN electrodes.

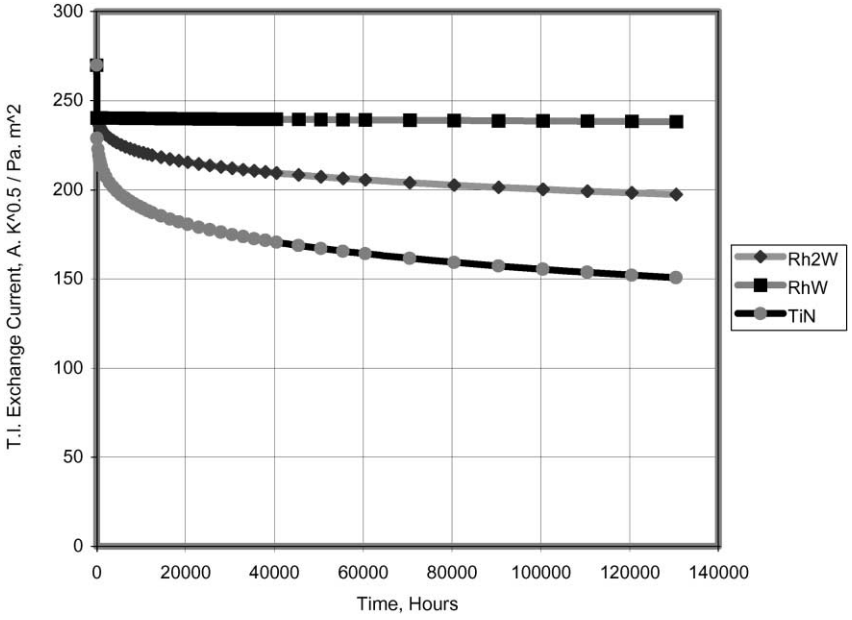

Fig. 3. The variation of temperature-independent exchange current with time for RhW, Rh_2W, and TiN electrodes.

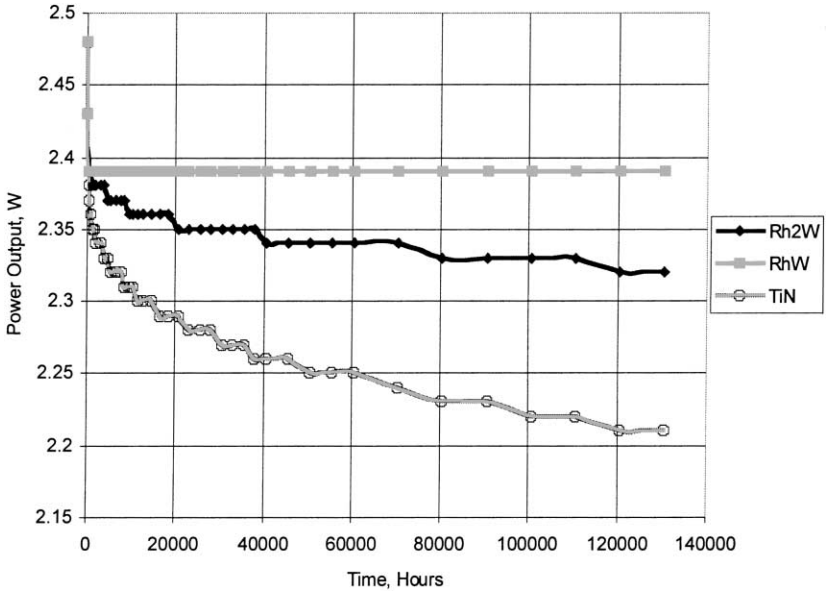

Fig. 4. The variation of power output with time for RhW, Rh_2W, and TiN electrodes.

of the temperature-independent exchange current and power output of all three electrodes are shown in Figs. 3 and 4.

Comparing the grain growth effect of all these electrode materials (Fig. 2), it is seen that grain size increases with time for all electrode materials investigated. Grain size of RhW electrode increased from 30 to 34.26 nm after 15 years, which is 1.142 times of its initial value. This implies that the RhW electrode is not significantly affected by the grain size effect. For Rh_2W and TiN electrodes, the grain size increased from 30 to 179.28 and 368.38 nm, respectively. The increase in the grain size of these materials was 6 and 12.28 times greater, respectively, from their original size of 30 nm.

From Fig. 3, it is seen that the temperature-independent exchange current of RhW, Rh_2W and TiN electrodes change in the 15 years time span, starting from the initial value of 270 A $K^{1/2}$/Pa $m^{1/2}$, for all three electrodes, it decreases to 238.26, 184.52, and 150.66 A $K^{1/2}$/Pa $m^{1/2}$, respectively, again affecting the RhW electrode least.

From the Fig. 4, it can be seen that power output of RhW, Rh_2W and TiN electrodes decreases with time. Power output decreases from 2.48 to 2.39, 2.32 and 2.21 W, respectively, for all three electrodes during their 15 years span. The changes in the power output, temperature-independent exchange current, and grain growth for all three electrodes over 15 years of time are shown in three different tables, namely, Tables 2–4, respectively.

Table 2
Parameters of TiN electrode

	Grain size (nm)	Temperature-independent exchange current (A $K^{1/2}$/Pa $m^{1/2}$)	Simulated power output (W)
Initial value	30.00	270.00	2.48
Final value after 15 years	368.38	150.66	2.21
Total change	338.38	119.34	0.27
Change (%)	1127.9	44.20	10.88

Table 3
Parameters of RhW electrode

	Grain size (nm)	Temperature-independent exchange current (A $K^{1/2}$/Pa $m^{1/2}$)	Simulated power output (W)
Initial value	30.00	270.00	2.48
Final value after 15 years	34.26	238.26	2.39
Total change	4.26	31.74	0.09
Change (%)	14.20	11.76	3.63

Table 4
Parameters of Rh_2W electrodes

	Grain size (nm)	Temperature-independent exchange current (A $K^{1/2}$/Pa $m^{1/2}$)	Simulated power output (W)
Initial value	30.00	270.00	2.48
Final value after 15 years	179.28	184.52	2.32
Total change	149.28	85.48	0.16
Change (%)	497.60	31.66	6.45

5. Conclusions

Electrode is one of the components, which contribute to the overall degradation of the power output of the AMTEC. Electrode material has an effective life after which the output of the electrode does not comply with the minimum requirement of the power output of AMTEC. Three electrodes made of RhW, Rh_2W, and TiN have been examined for degrading effects on the AMTEC power output. From this analysis, RhW is found to be the best working electrode, in the sense that it is least affected by the grain growth. Rh_2W is found to be the other better electrode compared to TiN electrode. From the comparison of grain growth, it was found that grain size of RhW is the least among all three electrodes.

From the power output–time analysis, it is observed that power degradation of RhW electrode is 3.63% from grain growth effect. Power degradation by Rh_2W and TiN electrodes are 6.45 and 10.89%, respectively, due to grain growth. This result is consistent considering that RhW, Rh_2W, and TiN have activation energy of 260.51, 206.48, and 175 kJ/mol, respectively. This activation energy implies that RhW electrode faces greater energy barrier towards the grain growth when compared with the Rh_2W electrode, whereas Rh_2W electrode faces greater energy barrier towards the grain growth when compared with the TiN electrode. Besides, rhodium is alloyed with tungsten in equal proportion in RhW electrode, whereas the ratio of rhodium with tungsten (W) is 2 in the Rh_2W electrode. Tungsten is a high melting point material, which implies that tungsten is less susceptible to the sintering. As RhW has more proportionate tungsten than the Rh_2W electrode, therefore, it is better electrode than the latter one. It may, however, be borne in mind that all the comparisons made in this study are based on the grain of the electrode material only.

Acknowledgements

We are indebted to John Merrill of Air Force Research Lab (AFRL), Albuquerque, NM for providing the AMTEC data before publication. This work is supported in part by the Texas Higher Education Coordinating Board Advanced Technology Program under Grant no. 003644-091, and AFOSR Sub-contract no. 99-0832 CFDA #12,800.

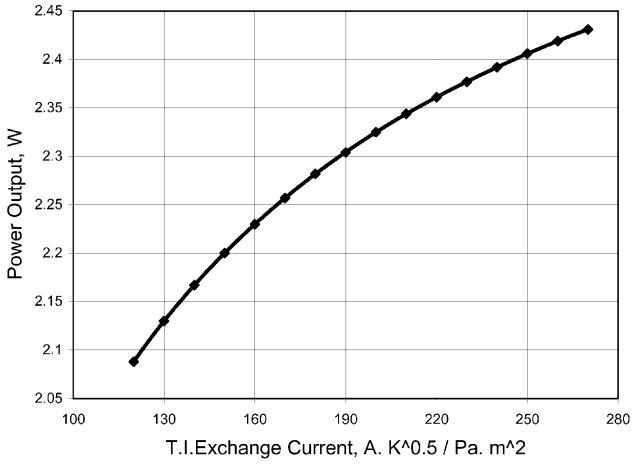

Fig. 5. The power output against temperature-independent exchange current of AMTEC. From this plot, an empirical relation has been obtained between the power output and temperature-independent exchange current given by $P_e = 1.5135 + 0.006B - 10^{-(1/2)B^2}$.

Appendix A

A simulation study has been set up with an 18,000-line FORTRAN code to study the variation in the power output of AMTEC with the change of values of different parameters. The description of the simulation is presented in [2,3], and relevant references cited therein. The simulation shows that power output increases with the increase of temperature-independent exchange current of cathode. The relation between the power output and temperature-independent exchange current is given in Fig. 5.

References

[1] Merrill John, AFRL, Albuquerque, NM, personal communication.
[2] M.A.K. Lodhi, P. Vijayaraghavan, A. Daloglu, Time-dependent BASE performance and power degradation in AMTEC, J. Power Sources 93 (2001) 41.
[3] M.A.K. Lodhi, M.S. Chowdhury, The role of electrodes in power degradation of AMTEC: their analysis and simulation, J. Power Sources 96 (2001) 369.
[4] T.K. Hunt, N. Weber, T. Cole, Research on the sodium heat engine, in: Proceedings of the 13th Intersociety Energy Conversion Engineering Conference, SAE, Warrendale, PA, 1978, p. 2011.

[5] R. Mital, et al., Performance Evaluation of Gas Fired AMTEC Power Systems, Advance Modular Power Systems Inc., USA, 1998, p. 1–2.
[6] M.A. Ryan, et al., Directly deposited current collecting grids for alkali metal thermal-to-electric converter electrodes, J. Electrochem. Soc. 142 (1995) 4252–4256.
[7] R.K. Sievers, C.P. Bankston, Radioisotope powered alkali metal thermoelectric converter design for space systems, in: Proceedings of the 23rd IECEC, 1988, p. 3.
[8] R.M. Williams, et al., Kinetics and transport at AMTEC electrodes. Part I. The interfacial impedance model, J. Electrochem. Soc. (Honolulu) 137 (1990) 1709–1715.
[9] T. Cole, Thermoelectric energy conversion with solid electrolytes, Science 221 (1983) 915–920.
[10] M.A. Ryan, et al., Advances in Materials and Current Collecting Networks for AMTEC Electrodes, JPL, California Institute of Technology, 1992, pp. 3.7–3.11.
[11] V.B. Shields, et al., Model for grain in AMTEC electrodes, in: Proceedings of the Intersociety Energy Conversion Engineering Conference, New York, 1999, pp. 1–3.
[12] R.M. Williams, et al., Kinetics and transport at AMTEC electrodes. Part II. Temperature dependence of the interfacial impedance of Na_g/porous Mo/Na-beta alumina, J. Electrochem. Soc. (Honolulu) 137 (1990) 1716–1722.
[13] M.A. Ryan, et al., Lifetimes of AMTEC electrodes: molybdenum, rhodium–tungsten, and titanium nitride, in: M.S. El-Genk (Ed.), Space Technology and Applications International Forum-2000, Vol. 2, 2000, pp. 1377–1382.